

## Density and Diffusion Anomalies in a repulsive lattice gas

Andressa A. Bertolazzo and Marcia C. Barbosa

*Instituto de Física, Universidade Federal do Rio Grande do Sul,  
Caixa Postal 15051, 91501-970, Porto Alegre, RS, Brazil*

### Abstract

We study a purely repulsive lattice gas model. The chemical versus temperature phase diagram is obtained using Grand Canonical Monte Carlo and Wang-Landau algorithms. This system exhibits a gas, two liquid phases and a high temperature fluid phase. In addition to the phase space we also explore this isotropic model for the presence of density and diffusion anomalies. We show that in the vicinity of the critical line between the fluid and the low density liquid phase the system exhibits temperatures of maximum density, minimum density, maximum diffusion and minimum diffusion in a behavior quite similar to the behavior observed in liquid water. Our results indicate that directionality and the presence of attractive interactions are not fundamental for the presence of water-like anomalies. phases.

© 2014 Elsevier B.V. This is an open access article under the CC BY-NC-ND license (<http://creativecommons.org/licenses/by-nc-nd/3.0/>).

Peer-review under responsibility of The Organizing Committee of CSP 2013 conference

**Keywords:** Wang-Landau algorithm, GCMC algorithm, lattice gas, anomalies

**PACS:** 05.10.Ln, 61.20.Ja, 64.60.Cn

### 1. Introduction

Water is the most anomalous substance in nature. Most liquids contract on cooling. Water exhibits a region of temperatures in which it expands on decreasing the temperature and at ambient pressure it has a maximum density at 4°C [1]. In addition to the density anomaly, the mobility of liquid water is quite unusual. In a normal liquid the diffusion coefficient,  $D$ , at constant temperature increases with the decrease of the pressure, since mobility is enhanced in a less dense medium. However, in the case of liquid water, a range of pressures exists for which diffusivity exhibits non monotonic behavior with pressure [2]. There are a density interval  $\rho_{Dmax} < \rho < \rho_{Dmin}$  in which  $D$  increases with increasing density [3].

From the microscopic point of view water anomalies have been interpreted qualitatively in terms a hydrogen bond network that form open and close structures that compete [4]. The simplest framework to test the hypothesis that the anomalies of water derive from the competition between bonding and non bonding structures are lattice models. A variety of statistical have been proposed for reproducing the anomalies of liquid water [5, 6, 7, 8, 9, 10, 11, 12, 13]. In addition to the occupational degree of freedom they also have an orientational variable. The anomalies appear due to the competition between these two degree of freedom. These models also exhibit an attractive interaction represented by the orientational variable. Is directionality essential for the presence of anomalies in lattice models? In order to address this question we propose a lattice model in which no directional interaction is present. The model also is represented by a single occupational variable and the interactions are purely repulsive. This model is tested for the presence of density and diffusion anomalies. In the sec. II this model is presented, in sec. III the Monte Carlo method employed for obtained the thermodynamic and dynamic properties of this model are shown and sec. IV presents our results. Conclusions are summarized in sec. V.

## 2. The Model

We considered a two dimensional lattice gas model in a triangular lattice with  $L^2$  sites. Each lattice site can be empty or occupied by a particle and each site has six nearest neighbors with a distance 1 and six next to nearest neighbors with distance  $\sqrt{3}$  in units of length. The particles interact by a two-scale repulsive potential: an infinite repulsive hard core interaction with its nearest neighbors and a finite repulsive interaction with its next to nearest neighbors. Therefore, if a site is occupied by a particle, its six nearest neighbors must be all empty and this particle will interact with its six next to nearest neighbors if they are occupied [14]. The Hamiltonian for this model is given by:

$$\tilde{\mathcal{H}} = \frac{1}{2} \sum_{i=1}^N \epsilon \sum_{\langle i,j \rangle} n_i n_j \quad (1)$$

where  $\langle i, j \rangle$  indicates the interaction of next to nearest neighbor pairs of sites,  $n_i$  is zero if the site  $i$  is empty and 1 if it is occupied,  $\epsilon > 0$  and in this work we consider  $\epsilon = 1$ .  $N$  is the number of occupied sites in the lattice. In the Grand Canonical Ensemble, we write an effective Hamiltonian, namely

$$\mathcal{H} = \frac{1}{2} \sum_{i=1}^N (\epsilon \sum_{\langle i,j \rangle} n_i n_j - \mu n_i) \quad (2)$$

And the grand potential will be defined as:

$$\Phi(T, \mu) = \langle \tilde{\mathcal{H}} \rangle - TS - \mu N \quad (3)$$

For  $T = 0$  there are three structures depending on the value of the chemical potential,  $\mu$ . For negatives values of chemical potential, the the grand potential is minimal for the empty lattice, no sites are occupied and we say that the system is in the gas phase. For intermediate values of chemical potential, positive but not so high, there is a competition between the chemical potential, that tends to fill the lattice, and the free energy, that is repulsive and tends to empty the lattice. Thereby, for  $0 < \mu < 12\epsilon$ , the system is in a configuration where a quarter of the lattice is occupied and there is no interaction between pairs of next to nearest neighbors, only the third-nearest neighbors are occupied in this configuration. We called this phase  $T4$ . For high enough chemical potential,  $\mu > 12\epsilon$ , the chemical potential term is more relevant and the system is in it maximum occupation, a third of the lattice is occupied and each particle has its six next to nearest neighbors occupied. This phase we called  $T3$ . Figure 1 illustrates the phases  $T3$  and  $T4$ . For different values of temperature we can observe three different phases: a disordered one and the other two ordered phases  $T3$  and  $T4$ . In order to understand the behavior of this model, for other values of temperature, we made use of numerical tools, such as Monte Carlo simulations. In the next section We are going to describe the method we used to study this system.

## 3. The Method

In order to understand the behavior of this model in the temperature vs chemical potential phase diagram, we made use of two different kinds of Monte Carlo simulations: the Wang-Landau algorithm [15, 16, 17, 18] and the Grand Canonical Monte Carlo algorithm (GCMC) [19].

### 3.1. Wang-Landau Algorithm

The Wang-Landau algorithm estimates the density of states,  $g(N, E)$ , that give us the number of states in a configuration of number of particles and energy. With this distribution the grand partition function is obtained by:

$$\Theta = \sum_{N,E} g(N, E) e^{-\beta(E - \mu N)}. \quad (4)$$

This algorithm made use of a flat-histogram random walk. We start the simulations setting all entries  $g(N, E) = 1$ , for all possible numbers of particles ( $N_i = 0, 1, \dots, L^2/3$  - where  $M = L \times L$  is the size of the square lattice) and energy.

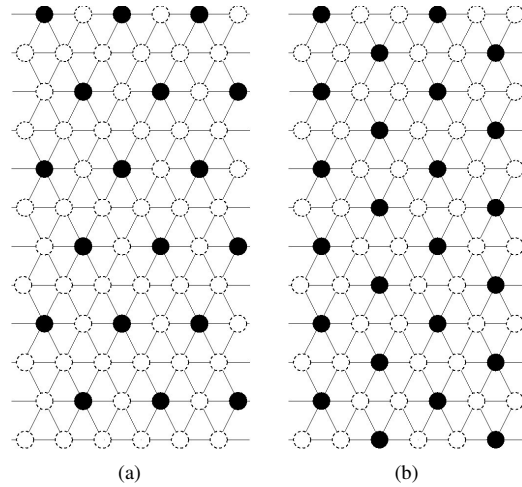


Figure 1: Representation of structures (a)  $T4$  and (b)  $T3$ . The structure  $T4$  have no interactions between particles and its next to nearest neighbors, because it has only the third-nearest neighbors in its structure. The structure  $T3$  has all nearest neighbors occupied and is the structure of maximum occupation in the lattice.

Then we begin with the random walk on  $(N, E)$  space. Since the probability for a state  $A(N_i, E_i)$  is proportional to  $1/g(A)$ , we set the transition probability from a state  $A$  to  $A'$  as:

$$p(A \rightarrow A') = \min\left(\frac{g(A)}{g(A')}, 1\right) \quad (5)$$

The lattice is composed of  $L^2$  sites with periodic boundary conditions. If a site is occupied the variable  $n_i = 1$ , otherwise the variable is zero. In this simulation we employ three kinds of movements: a particle can move to an available site, a new particle can be inserted in an available site or a particle can be removed. These movements will be accepted or not depending on the transition probability, Eq. (5). Each time in which a configuration  $A$  is visited, the density of states  $g(A)$  is modified by a modification factor  $f$ ,  $f > 1$ , so  $g(A) \rightarrow g(A) * f$ , and the histogram is updated with one more visit to the configuration  $A$ . This process is continued until the histogram is almost flat, i.e. until it obeys the flat rules in the simulation. When the simulation is considered flat, the histogram is reset and the factor  $f$  is modified:  $f \rightarrow \sqrt{f}$ . These steps are repeated until the modification factor  $f$  is smaller than a predefined value, such as  $f_{final} = \exp(10^{-8})$  in our simulation.

For the implementation of this algorithm, instead of the variables  $g(A)$  and  $f$ , the natural logarithm of these two quantities were used to be able to fit in double precision variables. We initialized  $f_0 = e^1$ .

The histogram is checked every  $10^4$  Monte Carlo steps by the rule that each histogram value can not fluctuate more than 10% of the average histogram value. At the end of simulation the parameters of the system are normalized considering that there is only one state when  $N = 0$  and  $E = 0$ , so all density states are divided by  $g(0, 0)$ . Using the values of  $g(N, E)$  we can calculate Grand Potential, namely

$$\Phi = -k_B T \ln(\Theta) . \quad (6)$$

From the Grand Potential it is possible to obtain all the thermodynamic properties such as the internal energy and the average number of particles in the system, respectively

$$U(T, \mu) = \frac{\sum_{\{N, E\}} E g(N, E) e^{-\beta(E - \mu N)}}{\sum_{\{N, E\}} g(N, E) e^{-\beta(E - \mu N)}} \quad (7)$$

$$\langle N \rangle = \frac{\sum_{\{N,E\}} Ng(N, E)e^{-\beta(E-\mu N)}}{\sum_{\{N,E\}} g(N, E)e^{-\beta(E-\mu N)}} . \quad (8)$$

From the quantities obtained with equations (7) and (8) it is possible to calculate the Specific Heat at constant volume, given by

$$c_V^* = \frac{C_V}{Vk_B} = \frac{\beta^2}{V} \left( \langle \delta H^2 \rangle_{\mu VT} - \frac{\langle \delta H \delta N \rangle_{\mu VT}^2}{\langle \delta N^2 \rangle_{\mu VT}} \right) + \frac{3}{2} \frac{N}{V} \quad (9)$$

The behavior of Eq. (8) versus temperature for fixed chemical potential allow us to check if this model exhibits the density anomaly observed in water.

### 3.2. Grand Canonical Monte Carlo Algorithm

The Grand Canonical Monte Carlo Algorithm was applied both to understand the behavior of this model in the temperature vs chemical potential phase diagram and to analyze the particle diffusion. The number of particles is variable and the average number of particles is determined by the thermal and chemical equilibrium. As in the Wang-Landau algorithm, the lattice is represented by a matrix, where sites can be occupied or empty. If a site “ $i$ ” is occupied, then  $n_i = 1$ , if it is empty,  $n_i = 0$ . At each Monte Carlo step a random site is chosen, if it is occupied it can be released depending on the transition of state probability. The change in the energy by adding a new particle is

$$\Delta \mathcal{H} = e_{empty} - e_{full} + \mu . \quad (10)$$

If this variation is negative or equal to zero, the site becomes empty with probability 1, otherwise, if it is positive, a random number is generated between  $[0,1]$  and if this number is less then  $\exp(-\beta\Delta\mathcal{H})$ .

After equilibrium stage, we measure the thermodynamic and dynamic quantities. For a fixed temperature and chemical potential we made several measures of energy and density. Between to measurements we iterate a number  $D = 200$  Monte Carlo steps without save data in order to descorrelate the obtained measurements.

The average of this quantities are used to analyze the thermodynamic properties of the system. The Monte Carlo method is considered atemporal, however, in order to analyze the dynamical properties for this model, we consider each Monte Carlo step as a time unit. The simulation starts with fixed temperature and chemical potential, it is initialized and iterated until its equilibrium state is reached. Then, we fixed the number of particles and we observed how is the diffusion of the particles in the lattice as a function of time (Monte Carlo steps). With the behavior of particles diffusion we obtained the diffusion constant as a function of system density.

At each Monte Carlo step the following procedure is repeated  $N$  times, where  $N$  is the number of particles in the lattice: the simulation chooses an random particle of the  $N$  occupied sites, after that, one of it six nearest neighbors is chosen, we know that all its six neighbors are empty. If this nearest neighbors has its six nearest neighbors empty (not considering the particle site itself), the particle can move with probability  $\exp(-\beta\mathcal{H})$ , otherwise the movement is rejected. We perform an average of  $n = 150$  samples to obtain  $\langle \Delta r^2 \rangle$ , namely

$$\langle [\Delta r(t)]^2 \rangle = \frac{1}{n} \sum_{i=1}^n [r_i(t) - r_i(0)]^2 \quad (11)$$

Considering the Einstein relation to great times,

$$\langle \Delta r(t)^2 \rangle = 4Dt \quad (12)$$

it is possible to obtain the translational diffusion coefficient  $D$  by measuring the slope of the linear curve of  $\langle \Delta r(t)^2 \rangle$  as a function of time. The factor 4 on equation (12) refers to a bi-dimensional system.

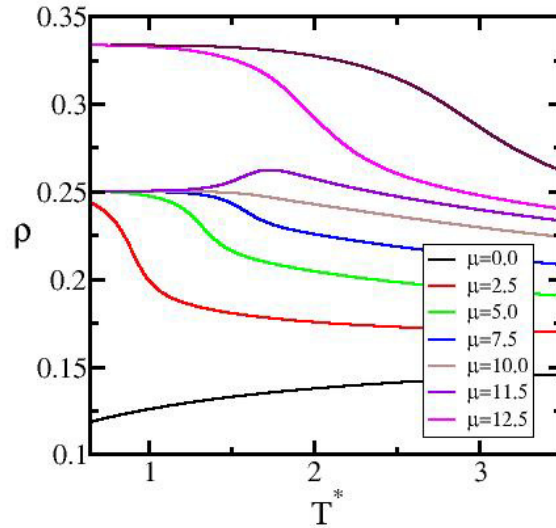


Figure 2: Variation of density by temperature changes for different fixed chemical potential values.

#### 4. The Results

In this section we test if a lattice model with no directional interaction and only repulsive interactions has the density and diffusion anomalous behaviors observed in water. First, we analyze how density changes when the temperature is increased, for a fixed value of chemical potential. Fig. 2 illustrates our results obtained using Wang-Landau algorithm. For  $\mu^* < 0$  the density increases with the temperature and reaches a value lower than the density of  $T4$  phase, indicating that the system is in the gas phase. For positive but small values of chemical potential,  $0 \leq \mu^* \leq 12$  the system at low temperatures is in the  $T4$  phase,  $\rho^* \approx 0.25$ . With the increase of temperature it undergoes a phase transition to a disordered phase with density lower than  $T4$ . For higher values of chemical potential,  $\mu^* > 12$ , for low temperatures the system is in the  $T3$  phase,  $\rho^* = 1/3$ . As the temperature is increased it undergoes a phase transition to the disordered phase.

For intermediate values of chemical potential,  $10.5 < \mu^* < 12$ , density at low temperature is in the  $T4$  phase but as the temperature is increased, it undergoes a phase transition to a disordered phase, however instead of a monotonic increase in the temperature it has an increase followed by a decrease of density with temperature, showing a temperature of maximum density.

For  $10.5 < \mu^* < 11.2$  in addition to the maximum in the density it also has a minimum in the density. This behavior is illustrated in figure 3. For  $11.2 \leq \mu^* < 12.0$ , as illustrated in the figure 4 only the maximum in the density is observed.

The TMD (temperature of maximum density) line observed in this lattice model was also seen in other directional lattice models [20] in which attractive interactions were present.

In addition to the density anomaly we also explore this model for the presence of diffusion anomaly. For this analysis we did employ the Grand Canonical Monte Carlo algorithm. With this algorithm it was possible to obtain the mean square displacement as a function of time, Monte Carlo steps, as illustrated in figure 5. For a fixed density, chemical potential and temperature, we can say that the system diffuses normally, because the  $\langle r^2 \rangle$  vs  $t$  is a linear curve. With this result it is possible to obtain the diffusion coefficient using equation 12 and the angular coefficient of these curves.

For a normal fluid at constant temperature, the diffusion coefficient decreases with the increase of density. Figure 6

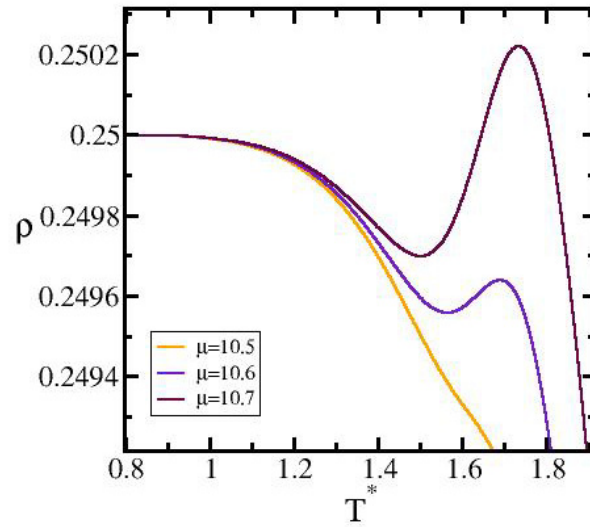


Figure 3: For some values of fixed chemical potential it is possible to observe an anomalous behavior in density by varying the temperature, such as for  $\mu = 10.6$  and  $\mu = 10.7$  in this figure, where we can see that density increases anomalously when temperature increases too. Furthermore, it is possible observe that density reaches a minimum and a maximum value in these cases.

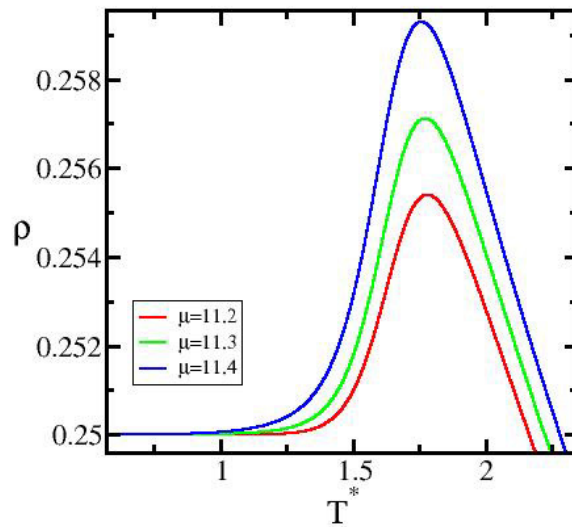


Figure 4: For some values of fixed chemical potential, density as function of temperature presents a maximum value and does not presents a minimum. This increase in density by an increase in temperature is a anomalous behavior, such as water ones.

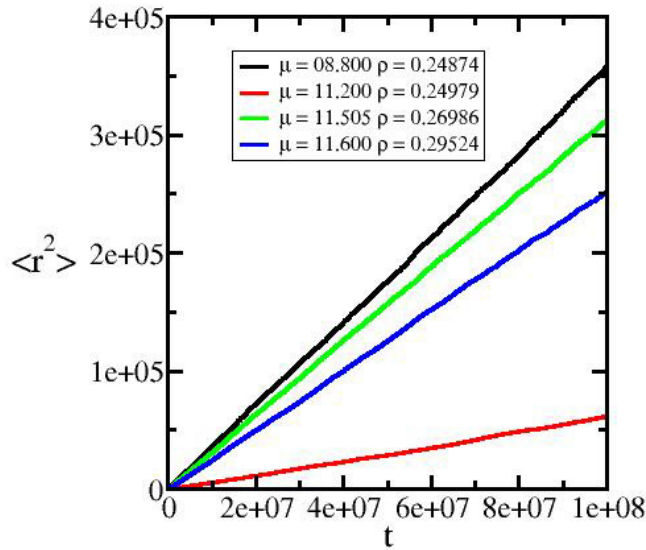


Figure 5: Mean square displacement as a function of time, Monte Carlo steps, for fixed chemical potential and density.

illustrates the diffusion coefficient versus density at constant temperatures for our model. For temperatures  $T^* = k_B T$  between  $1.35 \leq T^* \leq 1.60$  the diffusion coefficient decreases as density increases until it reaches a minimum, then it starts to grow until it reaches a maximum and then it decreases monotonically again. This anomalous behavior was found for different lattice models, as described in the introduction section. The same result was observed in directional lattice models in which attractive interaction were present [21]

The density and diffusion anomalous regions are illustrated in the pressure versus temperature phase diagram in figure 7. These two anomalies are located in the re-entrant region of phase transition from  $T4$  to the disordered phase, near to the  $T4$ - $T3$  transition.

Another information that we can obtain from figure 7 is the comparison of Wang-Landau and Metropolis algorithms for  $T4$ -disordered phase transition and for the density anomaly. In this figure the dark blue curve represents data from Metropolis algorithm for a  $M = 24 \times 24$  lattice, dark green curve represents data from Wang-Landau algorithm for a  $M = 6 \times 6$  lattice and pink curve represents data from Wang-Landau algorithm for a  $M = 12 \times 12$  lattice. As we see in this figure the smoothest curve is the pink one, made with data from Wang-Landau algorithm for a  $M = 12 \times 12$  lattice. Figure 8 is a zoom of figure 7 that only shows data from anomalous density position in phase diagram for both algorithms. The light green and violet curves are the location of minimum on density for Wang-Landau and Metropolis Algorithms, respectively. The brown and orange curves represent the maximum on density for Wang-Landau and Metropolis Algorithms, respectively. As we can see in this figure, results from Wang-Landau are closer to to Metropolis ones but are smoothest then the other one.

## 5. Conclusions

In this paper we have shown that even a purely repulsive and non directional model can exhibit both the density and the diffusion anomalies present in water. The major ingredient for the presence of the anomalies is the competition between two length scales defined in this potential by the infinite exclusion and the repulsive interaction against the chemical potential that induces filling the system with particles.

This system allow us to compare the two types of algorithms, Wang-Landau with Grand Canonical Metropolis Algorithm. The curves obtained using the Wang-Landau method, particularly in the low temperature phases, were

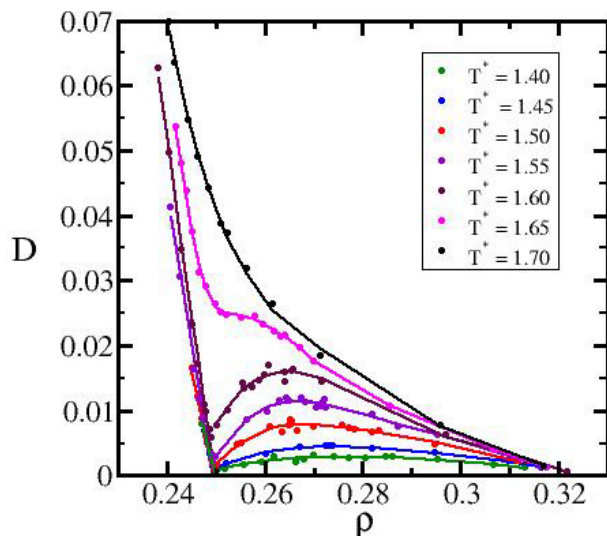


Figure 6: Diffusion coefficient, obtained with equation (12) by measure the angular coefficient of mean square displacement vs time curves - figure 5, as a function of system density.

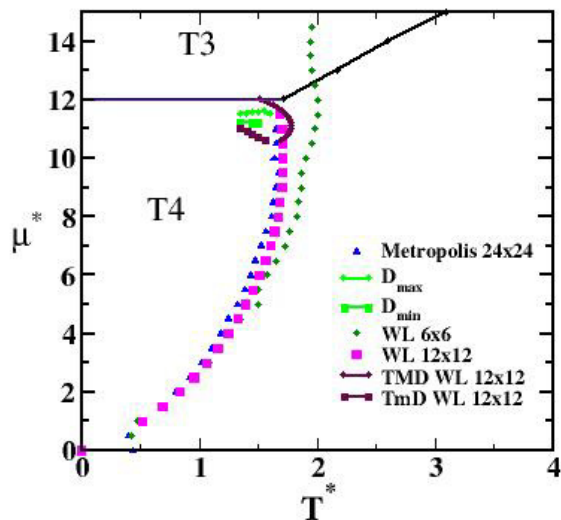


Figure 7: Temperature vs chemical potential phase diagram. The black lines represent phase transition that were measured with Metropolis algorithm for  $M = 24 \times 24$ . The phase transition between  $T4$  and the disordered phase can be compared by the two methods: the dark blue curve represents data from Metropolis algorithm for a  $M = 24 \times 24$  lattice, dark green curve represents data from Wang-Landau algorithm for a  $M = 6 \times 6$  lattice and pink curve represents data from Wang-Landau algorithm for a  $M = 12 \times 12$  lattice. The red and light green curves represent, respectively, minimum and maximum on diffusion coefficient. In figure 8 we plot a zoom for curves of density anomaly: light green, orange, brown and violet ones.



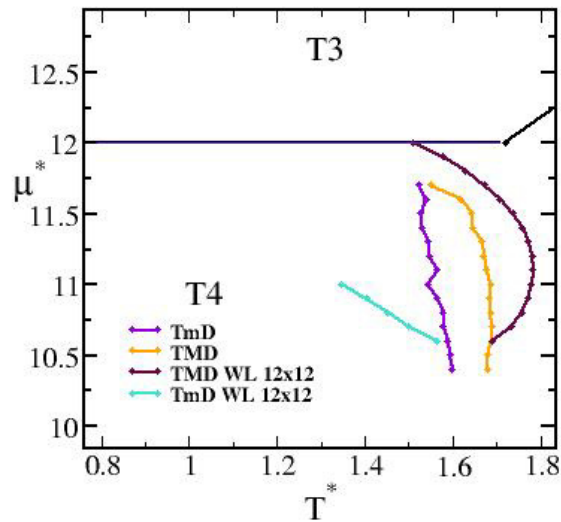


Figure 8: Zoom of the density anomaly region on phase diagram to compare the results of Wang-Landau and Metropolis algorithms. The light green violet curves are the location of minimum on density for Wang-Landau and Metropolis Algorithms, respectively. The brown and orange curves represent the maximum on density for Wang-Landau and Metropolis Algorithms, respectively.

more smooth.

## 6. Acknowledgment

We acknowledge Brazilian science agencies CAPES, CNPQ and INCT-FCx for financial support and Centro de Física Computacional - IF (CFCIF) for computational support.

## 7. References

- [1] G. S. Kell, *J. Chem. Eng. Data* **12**, 66 (1967).
- [2] H. E. Stanley, M.C. Barbosa, S. Mossa, P.A. Netz, F. Sciortino, F.W. Starr and M. Yamada *Physica A*, **315**, 281 (2002)
- [3] C. A. Angell and E. D. Finch and P. Bach, *J. Chem. Phys.* **65**, 3063 (1976).
- [4] J. D. Bernal and R. H. Fowler, *J. Chem. Phys.* **1**, 515 (1976).
- [5] S. Sastry, P. G. Debenedetti, F. Sciortino, and H. E. Stanley, *Phys. Rev. E* **53**, 6144 (1996).
- [6] G. Franzese, M. I. Marques, and H. E. Stanley, *Phys. Rev. E* **67**, 011103 (2003).
- [7] S. Sastry, F. Sciortino, and H. E. Stanley, *J. Chem. Phys.* **98**, 9863 (1993).
- [8] C. Buzano, E. De Stefanis and M. Pretti, *J. Chem. Phys.*, **129**, 024506 (2008).
- [9] V. B. Henriques, N. Guisoni, M. A. Barbosa, M. Thielo, and M. C. Barbosa, *Mol. Phys.* **103**, 3001 (2005).
- [10] C. E. Fiore, M. M. Szortyka, M. C. Barbosa, and V. B. Henriques, *J. Chem. Phys.* **131**, 164506 (2009).
- [11] M. Girardi, A. L. Balladares, V. Henriques, and M. C. Barbosa, *J. Chem. Phys.* **126**, 064503 (2007).
- [12] M. M. Szortyka, M. Girardi, V. Henriques, and M. C. Barbosa, *J. Chem. Phys.* **130**, 094504 (2009).
- [13] M. Szortyka, M. Girardi, V. B. Henriques and M. C. Barbosa, *J. Chem. Phys.* **132**, 134904 (2010).
- [14] N. G. Almaraz, J. A. Capitan, J. A. Cuesta, and E. Lomba, *J. Chem. Phys.* **131**, 124506 (2009).
- [15] F. Wang and D. P. Landau, *Phys. Rev. Lett.* **86**, 2050 (2001).
- [16] F. Wang and D. P. Landau, *Phys. Rev. E* **64**, 056101 (2001).
- [17] D. P. Landau and F. Wang, *Comp. Phys. Comm.* **147**, 674, (2002).
- [18] D. P. Landau and F. Wang, *Braz. J. Phys.* **34**, 354, (2004).
- [19] M. P. Allen and D. J. Tildesley, *Computer Simulations of Liquids* (Clarendon Press, Oxford, 1987), 1st ed.
- [20] M. M. Szortyka and M. C. Barbosa, *Physica A* **380**, 27 (2007).
- [21] M. Girardi, M. Szortyka, and M. C. Barbosa, *Physica A* **386**, 692 (2007);